

# Flavonoids for Controlling Starch Digestion: Structural Requirements for Inhibiting Human $\alpha$ -Amylase

Elena Lo Piparo,<sup>\*,‡</sup> Holger Scheib,<sup>‡</sup> Nathalie Frei, Gary Williamson, Martin Grigorov, and Chieh Jason Chou

Nestlé Research Center, Vers-chez-les-Blanc, P.O. Box 44, CH-1000 Lausanne 26, Switzerland

Received February 4, 2008

In this study we investigated the structural requirements for inhibition of human salivary  $\alpha$ -amylase by flavonoids. Four flavonols and three flavones, out of the 19 flavonoids tested, exhibited  $IC_{50}$  values less than 100  $\mu$ M against human salivary  $\alpha$ -amylase activity. Structure–activity relationships of these inhibitors by computational ligand docking showed that the inhibitory activity of flavonols and flavones depends on (i) hydrogen bonds between the hydroxyl groups of the polyphenol ligands and the catalytic residues of the binding site and (ii) formation of a conjugated  $\pi$ -system that stabilizes the interaction with the active site. Our findings show that certain naturally occurring flavonoids act as inhibitors of human  $\alpha$ -amylase, which makes them promising candidates for controlling the digestion of starch and postprandial glycemia.

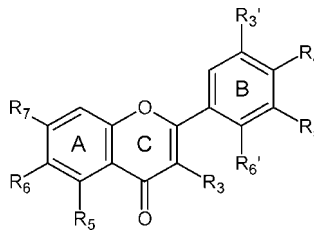
## Introduction

The process of carbohydrate digestion in mammals requires multiple enzymes functioning both sequentially and in parallel.  $\alpha$ -Amylase and two brush-border enzymes, malto-glucoamylase and sucrase-isomaltase, rapidly convert digestible starch into glucose monomers.  $\alpha$ -Amylases or  $\alpha$ -1,4-glucan-4-glucanohydrolases (EC 3.2.1.1) are endoglycosidases that belong to the glycosyl hydrolase family 13.<sup>1</sup> This family of proteins utilizes a double displacement catalytic mechanism in which a glycosyl enzyme intermediate is formed and hydrolyzed by acid/base catalysis via an oxocarbenium ion-like transition state.<sup>2</sup>  $\alpha$ -Amylases hydrolyze  $\alpha$ (1,4)-glucosidic linkages with retention of configuration at the sugar anomeric center.<sup>2</sup> In humans, there are five  $\alpha$ -amylase genes clustered in chromosome 1, at location 1q21. Three of them code for salivary  $\alpha$ -amylase, *AMY1A*, *AMY1B*, and *AMY1C*, and the other two genes *AMY2A* and *AMY2B* are expressed in the pancreas.<sup>3,4</sup> Both salivary and pancreatic  $\alpha$ -amylases are composed of 496 amino acids in a single polypeptide chain. Human salivary and pancreatic  $\alpha$ -amylases share a high degree of amino acid sequence similarity with 97% identical residues overall and 92% in the catalytic domains.<sup>5,6</sup>

Rapidly digested and absorbed dietary carbohydrates result in a sharp increase in the postprandial blood glucose level. For diabetic patients, the elevated blood glucose level after a meal presents a challenge for managing meal-associated hyperglycemia. Therefore, the inhibition of  $\alpha$ -amylase and  $\alpha$ -glucosidase by pharmaceutical agents such as acarbose is an accepted clinical strategy for managing postprandial glycemia in diabetic patients. Acarbose, a fermentation product of *Actinoplanes* species, has been shown to inhibit  $\alpha$ -amylase and  $\alpha$ -glucosidase competitively.<sup>7,8</sup> It is a pseudotetrasaccharide consisting of a polyhydroxylated aminocyclohexene derivative (valienamine) linked via its nitrogen atom to a 6-deoxyglucose, which is itself  $\alpha$ -1,4-linked to a maltose moiety.

Molecules present in plants have also been shown to inhibit  $\alpha$ -amylase. Results from clinical studies in humans showed that natural  $\alpha$ -amylase inhibitors isolated from wheat<sup>9</sup> and white

**Table 1.** Flavonol and Flavone Structures

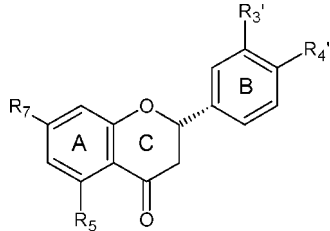


compd	group	R <sub>3</sub>	R <sub>5</sub>	R <sub>6</sub>	R <sub>7</sub>	R <sub>3'</sub>	R <sub>4'</sub>	R <sub>5'</sub>	R <sub>6'</sub>
fisetin	flavonol	OH	H	H	OH	H	OH	OH	H
kaempferol	flavonol	OH	OH	H	OH	H	OH	H	H
myricetin	flavonol	OH	OH	H	OH	OH	OH	OH	H
quercetagenin	flavonol	OH	OH	OH	OH	OH	OH	H	H
quercetin	flavonol	OH	OH	H	OH	OH	OH	H	H
isorhamnetin	flavonol	OH	OH	H	OH	H	OH	OCH <sub>3</sub>	H
ramnetin	flavonol	OH	OH	H	OCH <sub>3</sub>	OH	OH	H	H
acacetin	flavone	H	OH	H	OH	H	OCH <sub>3</sub>	H	H
diosmetin	flavone	H	OH	H	OH	OH	OCH <sub>3</sub>	H	H
eupafolin	flavone	H	OH	OCH <sub>3</sub>	OH	H	OH	OH	H
genkwanin	flavone	H	OH	H	OCH <sub>3</sub>	H	OCH <sub>3</sub>	H	H
luteolin	flavone	H	OH	H	OH	OH	OH	H	H
scutellarein	flavone	H	OH	OH	OH	H	OH	H	H

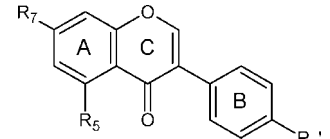
bean<sup>10</sup> significantly reduced the peak of postprandial glucose in healthy and type 2 diabetic subjects. Low molecular weight plant-derived molecules such as luteolin,<sup>11</sup> strawberry extracts,<sup>12</sup> and green tea polyphenols<sup>13,14</sup> have also been shown to inhibit  $\alpha$ -amylase or reduce postprandial hyperglycemia. Recently, Tadera et al. tested several flavonoid compounds for their inhibitory activity against  $\alpha$ -amylase.<sup>15</sup> They showed that luteolin, myricetin, and quercetin were potent inhibitors against porcine pancreatic  $\alpha$ -amylase and that the potency of inhibition correlated with the number of hydroxyl groups on the B ring of the flavonoid scaffold (Table 1). Yet it remains unclear how these results can be applied to the human variant of the protein, since 14% of the amino acids of the porcine and the human  $\alpha$ -amylases are different.<sup>5</sup> Therefore, we investigated the interactions between flavonoids and the human  $\alpha$ -amylase in order to understand the molecular requirements for enzyme inhibition to occur. Human salivary  $\alpha$ -amylase was chosen as a suitable enzyme for studying the structural requirements for the inhibitory activity of flavonoids by complementing in vitro

\*To whom correspondence should be addressed. Telephone: +41-(0)21-785-9530. Fax: +41-(0)21-785-9486. E-mail: elena.lopiparo@rdls.nestle.com.

<sup>‡</sup> These authors contributed equally to this work.

**Table 2.** Flavanone Structures


compd	group	R <sub>5</sub>	R <sub>7</sub>	R <sub>3'</sub>	R <sub>4'</sub>
hesperetin	flavanone	OH	OH	OH	OCH <sub>3</sub>
naringenin	flavanone	OH	OH	H	OH

**Table 3.** Isoflavone Structures


compd	group	R <sub>5</sub>	R <sub>7</sub>	R <sub>4'</sub>
genistein	isoflavone	OH	OH	OH
daidzein	isoflavone	H	OH	OH

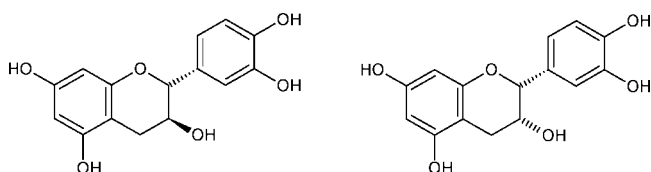
assays with in silico molecular modeling, giving insight into the molecular mechanisms of action of such inhibitors.

## Results

**In Vitro Study.** To identify candidate inhibitors, we used an in vitro assay for salivary  $\alpha$ -amylase with cooked potato starch as a substrate. Acarbose was used as a positive control, and its IC<sub>50</sub> value for inhibiting salivary  $\alpha$ -amylase was  $0.996 \pm 0.011 \mu\text{M}$ . We tested 19 molecules representing five families of natural flavonoids found in plants (Tables 1–3, Figure 1). Flavonoids share a common structural scaffold consisting of two aromatic rings (A and B) linked through three carbons, which, attached to the A-ring, form an oxygenated heterocycle (ring C). The five flavonoid subclasses studied (flavonols, flavones, flavanols, flavanones, and isoflavones) differ from each other with regard to (i) the type of heterocycle they contain as ring C, (ii) the substitution pattern of OH and OCH<sub>3</sub> groups at positions R<sub>3</sub>, R<sub>5</sub>, R<sub>6</sub>, and R<sub>7</sub> in the A–C condensate ring system as well as at positions R<sub>3'</sub>–R<sub>7'</sub> in ring B, and (iii) the position of the ring B (Tables 1–3, Figure 1).

Measurable inhibition was arbitrarily defined as an IC<sub>50</sub> value below  $100 \mu\text{M}$ . Our results showed that only compounds of the flavanol (quercetin, quercetagenin, myricetin, and fisetin) and flavone (luteolin, eupafolin, and scutellarein) families inhibited  $\alpha$ -amylase (Table 4). Maximum inhibition of salivary  $\alpha$ -amylase activity by quercetagenin, scutellarein, eupafolin, luteolin, fisetin, and quercetin was  $97.6 \pm 2.4\%$ ,  $98.4 \pm 1.6\%$ ,  $99.4 \pm 0.6\%$ ,  $88.8 \pm 7.2\%$ ,  $85.6 \pm 7.3\%$ , and  $82.1 \pm 4.6\%$ , respectively (Table 4).

**In Silico Study.** The in silico study was undertaken under the assumption that a predicted high docking score in absolute

**Figure 1.** Structures of the flavanols investigated: catechin (left side) and epicatechin (right side).**Table 4.** Experimental IC<sub>50</sub> Values and Maximum Inhibition as Well as the Glide and FLO+ Highest Docking Scores Results

family	IC <sub>50</sub> ( $\mu\text{M}$ )	maximum inhibition (%)	Glide (kcal/mol)	FLO+
acarbose	$0.996 \pm 0.011$	$99.2 \pm 0.5$	$-12.28$	5.1
quercetagenin	$10.2 \pm 2.2$	$97.6 \pm 2.4$	$-10.07$	5.7
fisetin	$19.6 \pm 6.4$	$85.6 \pm 7.3$	$-9.66$	5.3
quercetin	$21.4 \pm 4.3$	$82.1 \pm 4.6$	$-10.13$	6.5
myricetin	$30.2 \pm 2.9$	$79.0 \pm 7.5$	$-10.07$	5.5
kaempferol	ND	34.5	$-9.34$	5.4
isorhamnetin	ND	35.4	$-9.32$	4.8
rhamnetin	ND	8.1	$-8.67$	5.2
scutellarein	$9.64 \pm 0.30$	$98.4 \pm 1.6$	$-8.25$	5.6
luteolin	$18.4 \pm 3.9$	$88.8 \pm 7.2$	$-9.56$	5.9
eupafolin	$48.0 \pm 14.8$	$99.4 \pm 0.6$	$-9.67$	5.5
genkwanin	ND	17.5	$-8.89$	4.5
diosmetin	ND	19.2	$-8.63$	4.1
acacetin	ND	14.1	$-7.71$	4.6
catechin	ND	13.1	$-7.55$	4.7
epicatechin	ND	10.3	$-6.62$	4.5
hesperetin	ND	39.8	$-8.64$	4.4
naringenin	ND	26.8	$-7.82$	4.6
genistein	ND	25.1	$-7.97$	4.9
daidzein	ND	23.3	$-7.22$	5.1

value will be predictive of a strong inhibition of the enzyme. In this work, two conceptually different docking software (Glide and FLO+) were used. Whereas both programs allow full flexibility of the ligand, Glide treats the binding site as rigid (flexible ligand–rigid binding site) and FLO+ as flexible (flexible ligand–flexible binding site). This means that FLO+ in contrast to Glide can simulate movements of amino acid side chains upon ligand binding. Despite these differences, both docking programs yielded similar results except for scutellarein where FLO+ provided a better docking score (stronger binding) than Glide. Table 4 summarizes the experimental IC<sub>50</sub> values and the maximum inhibition for salivary  $\alpha$ -amylase as well as the highest docking scores obtained. FLO+ and Glide in general consensually predicted the same binding modes, indicating that the binding site does not undergo pronounced conformational changes upon binding of the ligand. Moreover, lowest docking scores were observed for flavanols, flavanones, and isoflavones, all of which are experimentally poor inhibitors of salivary  $\alpha$ -amylase (Table 4). In contrast, docking scores for flavonols and flavones were generally higher corresponding to stronger binding and thus to inhibition of salivary  $\alpha$ -amylase.

Our in silico studies revealed that OH groups present in position R<sub>7</sub> of the A ring and the ones contained in the B ring, especially in position R<sub>4'</sub>, are particularly important for inhibition to occur, whereas less essential interactions involved positions R<sub>3</sub> and R<sub>3'</sub>. Overall, the inhibitory activity of flavonoids toward human salivary  $\alpha$ -amylase depends on two parameters: (i) Can hydrogen bonds be formed between the OH groups in R<sub>7</sub> and R<sub>4'</sub> of the flavonoid and the side chains of Asp<sup>197</sup> and Glu<sup>233</sup>? (ii) Can a conjugated  $\pi$ -system be formed between the indole Trp<sup>59</sup> and the AC heterocyclic ring of the flavonoids?

In order to further compare docking results obtained with Glide and FLO+ to each other, the modified acarbose inhibitor was first extracted from the pancreatic  $\alpha$ -amylase crystal structure 1CPU and then computationally docked to salivary  $\alpha$ -amylase. All flavonoid docking modes obtained by Glide and FLO+ were then analyzed with acarbose as a reference. In the following, poses are described by using the established nomenclature for acarbose substructures first put forward for acarbose binding to pancreatic  $\alpha$ -amylase ( $-3 -2 -1 +1 +2$ ).<sup>2</sup> In general, the main docking conformation of flavonoids inhibiting

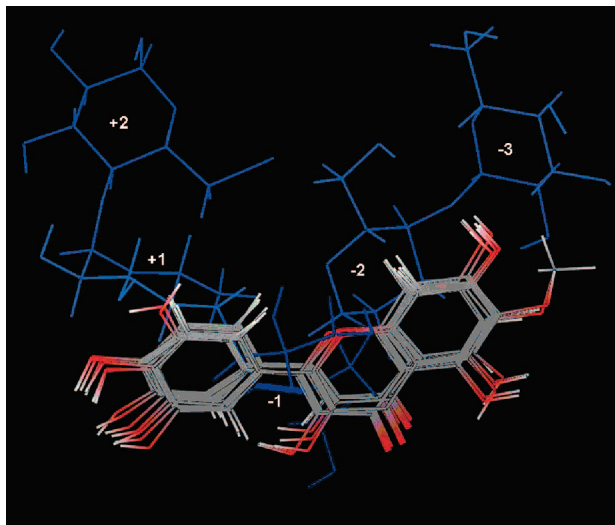


**Figure 2.** Superimposition of the main docking pose of active flavonoids (pose 1) with acarbose in human salivary  $\alpha$ -amylase.

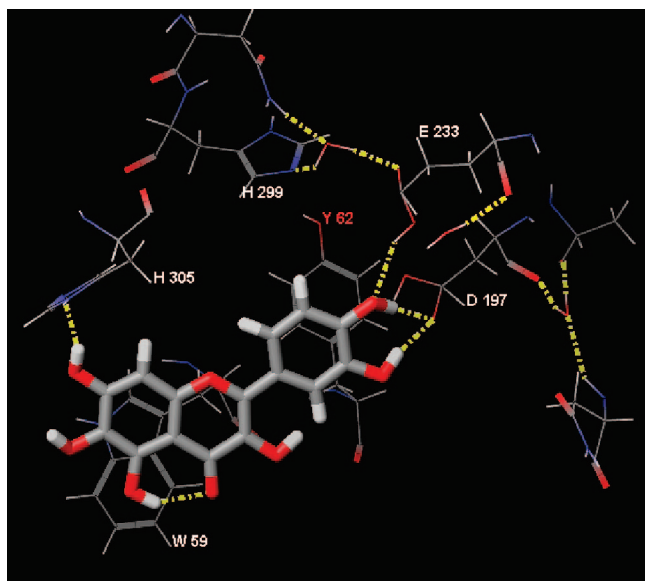


**Figure 3.** Pose 1: main binding mode of quercetagenin in the human salivary  $\alpha$ -amylase binding site.

salivary  $\alpha$ -amylase was similar to subsite  $-1$  of acarbose (pose 1, Figure 2).

**Flexible Ligand–Rigid Binding Site: Glide Results.** Our Glide docking studies revealed that a strong interaction between a flavonoid ligand and the enzyme resulted in one main docking mode (pose 1). In pose 1 the B rings of flavonol and flavanone inhibitors aligned on top of each other (Figure 2) and allow for efficient  $\pi$ – $\pi$  interactions with the aromatic side chain of Tyr<sup>62</sup> (Figure 3). Furthermore, in this binding mode the ligands interacted mainly with the catalytic residues in acarbose subsite  $-1$ : Two H-bonds were formed between the OH substituents in positions R3' and R4' of ring B and the carboxylate groups of Asp<sup>197</sup> and Glu<sup>233</sup>. An additional third H-bond was observed between the hydroxyl group in R7 of ring A and His<sup>305</sup>. However, from the position of the ligand in pose 1 we also postulate the presence of  $\pi$ – $\pi$  interactions between the AC-ring of the ligand and the indole ring of Trp<sup>59</sup>. All active inhibitors were found in the described binding pose 1, except for scutellarein, which gave a weaker Glide score than expected from in vitro experiments. The flavone-type inhibitor scutellarein

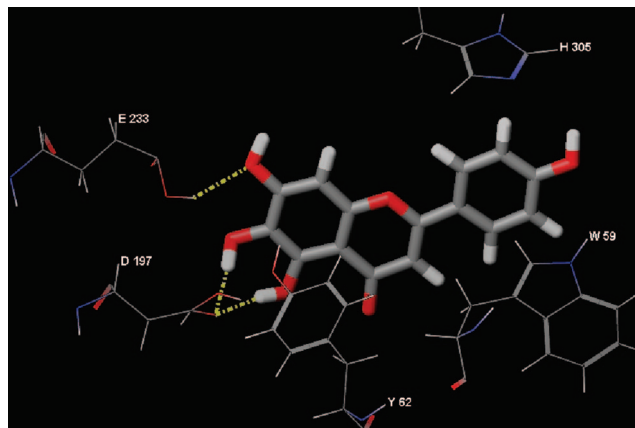


**Figure 4.** Pose 2: binding mode of scutellarein in the human salivary  $\alpha$ -amylase binding site.

preferentially interacted with salivary  $\alpha$ -amylase in an alternative mode (pose 2) (Figure 4). In pose 2 the ligand was flipped by 180° with respect to pose 1. Poses 1 and 2 can be distinguished by the aromatic ring system that interacts with the catalytic Asp<sup>197</sup> in subsite  $-1$ . In pose 1 the B-ring (Figure 3) interacts with Asp<sup>197</sup>, and in pose 2 the AC condensate ring system (Figure 4) interacts with Asp<sup>197</sup>. In pose 2 the ligand may form H-bonds from its OH-groups in R5, R6, and R7 of ring A to the side chains of Asp<sup>197</sup> and Glu<sup>233</sup>. Yet this pose only allowed for weaker  $\pi$ – $\pi$  interactions between Trp<sup>59</sup> and ring B, which we expect to be reflected in the weaker Glide docking score.

When Glide was used, it became possible to discriminate by in silico screening the family of flavonoids with good inhibitory activity from poor inhibitors family. The low docking scores for the poorly binding or nonbinding flavonoids result from weak binding interactions (Table 4). An analysis of the respective docking poses revealed that poorly binding or nonbinding ligands are geometrically aligned on the active ones (pose 1) but contain fewer hydroxyl group substituents to stabilize the interactions of the ligand with the protein. Another smaller fraction of the poorly binding or nonbinding ligands were predicted to bind to the amylase in a different mode compared to the active ones but still displayed much weaker interactions.

In more detail, the analysis of docking conformations of flavonol inhibitors versus noninhibitors revealed that kaempferol and isorhamnetin took up pose 1 when docked with Glide. Both ligands aligned well with the active inhibitors in the binding site but formed fewer H-bonds reflected in lower docking scores. The third poorly binding flavonol rhamnetin bound to salivary  $\alpha$ -amylase in pose 2, similar to scutellarein. Rhamnetin showed weaker interactions than the other flavonols because of the steric hindrance of the methoxy group at position R7, which in kaempferol and isorhamnetin is a hydroxyl group.

For the flavones with a methoxyl in R7 and/or R4' (acacetin, genkwanin, and diosmetin), both the inhibition and the in silico score decreased as a result of fewer hydrogen bonds that may be formed with the amino acids of the binding site. This effect was most prominent for acacetin, which does not contain any hydroxyl group in ring B; its docking score was comparable to the ones for flavanols, flavanones, and isoflavones. This suggests that interactions between the side chains of Asp<sup>197</sup>, Glu<sup>233</sup>, and His<sup>305</sup> and the hydroxyl groups in R3', R4', and R7 are of paramount importance for inhibition of salivary  $\alpha$ -amylase by flavonoids.

In contrast to flavonols and flavones, flavanols and flavanones do not possess a carbon–carbon double bond between C2 and



C3 of ring C, and as a consequence their C-ring is less electron-rich compared to flavonols and flavanones. The missing electrons lead to weaker  $\pi$ - $\pi$  interactions with the indole ring of Trp<sup>59</sup> and, eventually, to a reduced inhibitory activity of these compound classes toward human salivary  $\alpha$ -amylase. Moreover, isoflavones did not form H-bonds with the catalytic residues of human salivary  $\alpha$ -amylase, which is a likely consequence of the position of ring B; in isoflavones, as opposed to the other flavonoids studied, the B-ring is attached to carbon C3 rather than C2 of ring C.

**Flexible Ligand—Flexible Binding Site: FLO+ Results.** In contrast to Glide, in FLO+ any number of amino acids in the protein can be assigned side chain flexibility during docking. Such increased flexibility might lead to more docking poses than a flexible ligand—rigid binding site approach, since it allows the binding site to rearrange upon binding of a ligand. Generally, two docking poses were observed that were comparable to pose 1 and pose 2 observed during Glide docking. However, the flexibility of the binding site allowed for slight variations in the position of the ligands. Pose 2 appeared to be clearly preferred for scutellarein, which is in agreement with the Glide docking results. However, for quercetagenin and luteolin also an alternative orientation of the ligand in the binding site was observed, yet with slightly weaker docking scores. This shows that flavonols and flavones cannot be separated by their preferred docking mode. It was further observed that lower scoring docking solutions for salivary  $\alpha$ -amylase inhibitors allowed for a flip from pose 1 to pose 2 and vice versa. This indicates that even if a pose conformation is energetically preferred over another, the alternative pose conformation is not forbidden and could be populated.

Binding to salivary  $\alpha$ -amylase in pose 1 includes interactions of mainly R3' and R4' as well as R5' (B-ring) with Asp<sup>197</sup> and Glu<sup>233</sup> and in some cases also Asp<sup>300</sup>. With the exception of quercetin, which occupied pose 1 in a slightly distorted way, the ligands binding to salivary  $\alpha$ -amylase in pose 1 could all undergo possible  $\pi$ - $\pi$  interactions with the indole ring of Trp<sup>59</sup>. In pose 2, the OH moieties in R5, R6, and R7 (A-ring) interacted with Asp<sup>197</sup>, Glu<sup>233</sup>, and Asp<sup>300</sup>. For luteolin and quercetagenin, the carbonyl group in ring C accepted an additional H-bond from His<sup>299</sup>. Moreover, pose 2 did not favor formation of  $\pi$ - $\pi$  interactions with Trp<sup>59</sup>.

## Discussion

The scope of this work was to identify natural polyphenol inhibitors for human salivary  $\alpha$ -amylase and to investigate their mechanism of action. The inhibitory activity of 19 flavonoids toward salivary  $\alpha$ -amylase was determined both experimentally by in vitro assay and by computational ligand docking using two different docking software packages, namely, Glide and FLO+. Our in vitro and in silico results (Table 4) revealed that flavonoids strongly inhibit  $\alpha$ -amylase only if they contain common structural features. First, flavonols and flavones (the most active families) share a similar scaffold: a 4-oxo-flavonoid nucleus as C-ring. Molecules of both subclasses possess a carbonyl group at position C4 of the pyrone ring (Table 1). The C2—C3 double bond is conjugated to the 4-keto group and is responsible for electron delocalization between the benzopyrone (ring C) and the benzene ring (ring A). As a consequence, flavone and flavonol compounds form a highly conjugated  $\pi$ -system that confers better stability of the compound when binding to the active site of the enzyme. Second, a specific pattern of OH groups appears to be necessary for interactions with the enzyme. It was found here that hydroxyl groups in

position R6 or R7 of the A-ring and position R4' or R5' of the B-ring are favorable for the ligand to interact with the residues of the catalytic center, mostly with Asp<sup>197</sup> and Glu<sup>233</sup>. These results are in general agreement with the mechanism of action proposed for acarbose, since the importance of the partial planarity of valienamine and the presence of hydroxyl groups was proposed in that case.<sup>2</sup>

We showed that quercetagenin and scutellarein may function as two potent natural salivary  $\alpha$ -amylase inhibitors. Although quercetagenin and scutellarein belong to the groups of flavonols and flavones, respectively, the two molecules share common structural features with four hydroxyl groups at positions R5, R6, and R7 in the A ring and R4' in the B ring. Quercetagenin and scutellarein only differ in their substitution pattern of positions R3 and R3', where scutellarein lacks the two hydroxyl groups present in quercetagenin.

Our in silico studies further showed that OH groups present in positions R7 and R4' are particularly important for inhibition to occur, whereas less essential interactions involved positions R3 and R3'. Overall, the inhibitory activity of flavonoids toward human  $\alpha$ -amylase depends on the formation of (i) hydrogen bonds between the OH groups in R7 and/or R4' of the flavonoid ligand and the side chains of Asp<sup>197</sup> and Glu<sup>233</sup> and (ii) a possible conjugated  $\pi$ -system between either the AC- or B-ring system and Trp<sup>59</sup>.

**Comparison of the Interaction between Acarbose and Flavonoids.** Like most of the retaining glycosidases,  $\alpha$ -amylase utilizes active site carboxylic acids to catalyze the hydrolytic reaction. In particular, Asp<sup>197</sup>, Glu<sup>233</sup>, and Asp<sup>300</sup> were described to function as catalytic residues.<sup>2,2,16</sup> It has been suggested that Asp<sup>197</sup> was the nucleophile that attacks the substrate at the sugar anomeric center, forming a covalently bound reaction intermediate. In this step, the reducing end of the substrate is cleaved off the sugar skeleton. In a second step a water molecule attacks the anomeric center to break the covalent bond between Asp<sup>197</sup> and the substrate, attaching an OH group to the anomeric center. In both steps Glu<sup>233</sup> and Asp<sup>300</sup> either individually or collectively act as acid/base catalysts. As a consequence, the active site of human  $\alpha$ -amylase consists of several major binding subsites identified through kinetic studies. For the closely related human pancreatic  $\alpha$ -amylase, the cocrystallized acarbose inhibitor was described to bind subsites “-3” through “+2”.<sup>2</sup> In the same study it was reported that the “-1”, “-2”, and “-3” pocket is the core of the catalytic reaction and is more hydrophilic than the one spanning subsites “+1” and “+2” containing the leaving group. In acarbose the valienamine moiety is found in binding subsite -1 and its strong inhibition is believed to result from enhanced binding of this moiety with the side chain of Asp<sup>197</sup>, Glu<sup>233</sup>, and Asp<sup>300</sup>. Kinetic studies also highlighted the importance in catalysis of the presence of hydroxyl groups in the ligand together with the Asp<sup>197</sup>, Glu<sup>233</sup>, and Asp<sup>300</sup> residues in the binding site (substitution of these residues leading to a considerable drop in catalytic activity).<sup>2</sup> From the high overall sequence similarity the same can be confidently assumed for the binding site of salivary  $\alpha$ -amylase. Our results from studies on the inhibition of flavonoids are in general agreement with the mechanism of action proposed for acarbose, since they showed for salivary  $\alpha$ -amylase that active ligands exclusively occupy subsites “-1” and interact with the side chains of Asp<sup>197</sup>, Glu<sup>233</sup>, and Asp<sup>300</sup>. All strong inhibitors in this project occupied the binding site similar to valienamine and formed hydrogen bonds with residues of the catalytic site. In other words, the active ligands were anchored at the catalytic center subsite “-1”, which might explain why the enzymatic

activity of  $\alpha$ -amylase was successfully blocked. The other end of the ligand may form  $\pi$ - $\pi$  interactions of stacked delocalized ring systems of the ligand and the indole ring of Trp<sup>59</sup>. By contrast, ligands without inhibitory activity (flavanols, flavanones, and isoflavones) did not interact at the same time with the catalytic residues as well as with Trp<sup>59</sup>. Flavanols and flavanones possess a C2–C3 single bond that prevents electron delocalization over the A–C condensate ring system. Therefore,  $\pi$ -bonding may only occur between the benzene ring A or ring B and Trp<sup>59</sup> and would be expected to be weaker compared to flavanols and flavones. In contrast, the isoflavone genistein may form a  $\pi$ -bond to Trp<sup>59</sup> but was unable to form a hydrogen bond to the catalytic residues because of the different position of the aromatic B ring in the ligand structure. These findings suggest that hydrogen bonds between the catalytic residues and the dihydroxybenzopyran groups (ring A and ring B) are necessary but not sufficient to inhibit human  $\alpha$ -amylase.

**Natural Inhibitors for Human  $\alpha$ -Amylase.** Modulation of  $\alpha$ -amylase activity affects the utilization of carbohydrate as an energy source, sometimes drastically. Natural  $\alpha$ -amylase inhibitors have been known for many years and were discovered in plants, such as wheat and legumes.<sup>17,18</sup> Herbal medicines used to treat diabetes also contain substances with anti- $\alpha$ -amylase activity.<sup>19</sup> Several molecules from plants have been reported previously to inhibit  $\alpha$ -amylase. In this work, we confirmed quercetin<sup>20</sup> and luteolin<sup>11</sup> as functional  $\alpha$ -amylase inhibitors and we also described the inhibitory activities of flavonoids such as quercetagenin, myricetin, fisetin, scutellarein, and eupafolin that have been described very recently in the literature to inhibit porcine pancreatic  $\alpha$ -amylase.<sup>15</sup>

In salivary  $\alpha$ -amylase activity assays, acarbose was only 5 times more potent than the most active polyphenol inhibitor. On the basis of the efficacious dose for humans, it is possible to reduce  $\alpha$ -amylase activity by consuming food rich in polyphenols with strong  $\alpha$ -amylase inhibitory activity. However, available evidence for the efficacy of using natural  $\alpha$ -amylase to reduce starch digestion is still controversial.<sup>21</sup> Preserving the native structure of the active molecules during food preparation and ingestion is important before delivering these molecules to the small intestine where the most of the starch is hydrolyzed. Therefore, integration of flavonoid  $\alpha$ -amylase inhibitors in a well-designed food matrix with a given amount of starch load would be necessary to demonstrate the bioefficacy of the natural compounds. By understanding of the structure–function relationships between flavonoids and human  $\alpha$ -amylase, one could facilitate the discovery and development processes for designing a functional food for type 2 diabetic patients.

## Conclusion

The scope of this work was to identify natural polyphenol inhibitors against human salivary  $\alpha$ -amylase and to investigate their mechanism of action. Seven out of a total of 19 flavonoids studied showed some inhibition of salivary  $\alpha$ -amylase both in vitro and in silico, with quercetagenin and scutellarein showing the strongest inhibition in vitro. Our molecular modeling studies revealed that salivary  $\alpha$ -amylase inhibitors predominantly occupied a docking mode that allowed for H-bonds between the enzyme and hydroxyl groups in ring B of the flavonoid skeleton. Alternatively, the condensate AC-ring could H-bond to the residues of the active site. Strong inhibition of  $\alpha$ -amylase by acarbose is attributed to the presence of strong electrostatic interactions between the carboxyl groups at the active site and the protonated nitrogen of the inhibitor and to the partial planarity of valienamine. Interestingly, we found similar interac-

tions with the inhibitory flavonoids (hydrogen bonds formed between the hydroxyl groups of the polyphenol ligands and the catalytic residues of the binding site, and the planar condensate ring structure containing a 4-oxo-flavonoid nucleus that allows for formation of a highly conjugated  $\pi$ -system). The prominent feature among the contacts is a hydrogen bond formed between the Asp<sup>197</sup> side chain carboxyl oxygen atom and the hydroxyl group of flavonoid that mimics the glycosidic bond normally cleaved by  $\alpha$ -amylase. All these interactions are absolutely critical for the binding between flavonoids and the salivary  $\alpha$ -amylase isoform. Knowledge gained in this study would help future developments of functional foods for controlling starch digestion and postprandial glycemia.

## Experimental Section

**In Vitro Screening Assays.** Human salivary  $\alpha$ -amylase (type IX-A),  $\alpha$ -amylase inhibitor from *Triticum aestivum* (type III), copper sulfate pentahydrate, ammonium molybdate, sodium arsenate heptahydrate, sodium carbonate, sodium potassium tartrate, calcium chloride, bovine serum albumin, and genistein were obtained from Sigma Chemical Co. Sodium sulfate, sodium phosphate, and sodium chloride were obtained from Merck. (+)-Catechin, daidzein, diosmetin, (–)-epicatechin, fisetin, genkwanin, hesperetin, isorhamnetin, kaempferol, luteolin, naringenin, quercetin, quercetagenin, rhamnetin, myricetin, eupafolin, acacetin, and scutellarein were purchased from Extrasynthèse. Acarbose was obtained from SERVA Electrophoresis. A kit based on the Ceralpha procedure for measuring  $\alpha$ -amylase activity was purchased from Megazyme International Ireland Ltd.

The activity measurement of salivary  $\alpha$ -amylase was modified from a previous method.<sup>22,23</sup>  $\alpha$ -amylase was diluted in water on the same day of the experiment. Stock solutions for each compound tested (100 mM) were prepared in DMSO and stored at  $-20^{\circ}\text{C}$ . Working solutions at different concentrations were prepared immediately before a 30 min preincubation with salivary  $\alpha$ -amylase. A preincubation buffer contained 50 mM  $\text{NaH}_2\text{PO}_4$ /50 mM  $\text{NaCl}$ /0.5 mM  $\text{CaCl}_2$ /0.1% bovine serum albumin, pH 6.0. Test compounds were diluted with the preincubation buffer to the following final concentrations: 0, 0.1  $\mu\text{M}$ , 1  $\mu\text{M}$ , 10  $\mu\text{M}$ , 100  $\mu\text{M}$ , 1 mM, and 10 mM with  $\alpha$ -amylase at  $4 \times 10^{-4}$  mM. Potato starch was boiled for 15 min in a buffer containing 20 mM  $\text{NaH}_2\text{PO}_4$ /6.7 mM  $\text{NaCl}$ . Then the cooked potato starch was added to the preincubation solution to start the assay. The assay was carried out at room temperature for 10 min with salivary  $\alpha$ -amylase at  $1.8 \times 10^{-4}$  mM, starch at 0.15  $\mu\text{g}$ , and test compounds up to 0.888 mM, pH 6.0. The reducing sugar was determined by the Nelson–Somogyi procedure by measuring the absorbance at 540 nm.<sup>24</sup> The potency of the inhibition was determined by  $\text{IC}_{50}$  values and maximum percentage of inhibition.

**Molecular Modeling. Protein Structure Preparation.** We investigated the interactions of ligands with the human salivary  $\alpha$ -amylase using its X-ray structure deposited in the Protein Data Bank at Brookhaven under the reference code 1SMD.<sup>6</sup> It represents the apoform of the enzyme and hence was crystallized without an inhibitor present. The residues forming the binding site of 1SMD were selected by similarity to the binding site residues of human pancreatic  $\alpha$ -amylase. The pancreatic  $\alpha$ -amylase X-ray structure 1CPU<sup>2</sup> contains a modified form of the well-known  $\alpha$ -amylase inhibitor acarbose that was cocrystallized in the binding pocket. 1SMD and 1CPU were superimposed applying the SPDBV molecular modeling program,<sup>25</sup> and a residue in salivary  $\alpha$ -amylase was considered being part of the substrate binding site when it was located in the same position as the binding site residues in pancreatic  $\alpha$ -amylase. The salivary  $\alpha$ -amylase structure was prepared for docking by removing from the crystallographic structure ions and water molecules except the ones contained in the binding site (525, 557, and 646). Since the salivary  $\alpha$ -amylase X-ray structure does not contain hydrogen atoms, H-atoms were added to the enzymes by the respective docking programs (see below).

**Ligand Structure Optimization.** We designed and compiled a data set of 19 flavonoids (Tables 1–3 and Figure 1) that were selected from flavonols (seven examples), flavones (six examples), flavanols (two examples), flavanones (two examples), and isoflavones (two examples). By use of the Maestro 7.5 graphical interface,<sup>26</sup> the atomic structure of each molecule was built manually. The molecular mechanical energy of the ligands was minimized using the impact energy minimization option applying the OPLS\_2005 force field and the conjugate gradient algorithm with a maximum of 1000 cycles and 0.01 as gradient criterion.<sup>27</sup> Additionally, the modified structure of acarbose was extracted from the 1CPU X-ray structure and the double bond and hydrogen atoms were added.

Two well-established software packages, Glide (grid-based ligand docking with energetics)<sup>28–30</sup> and FLO+,<sup>31</sup> were used to perform the molecular docking calculations.

**Glide Docking.** The Glide docking program is based on a systematic sampling of ligand binding modes in conformational space using a series of hierarchical filters. The protein binding site is computed as a grid and is defined as a rectangular box. A fast site-point search generates initial ligand binding modes that are preliminarily scored. Solutions with higher scores are then selected for energy minimization on van der Waals and electrostatic grids that were precomputed applying the OPLS-AA (optimized potential for liquid simulations-all atom) force field.<sup>32</sup> The resulting lowest energy binding modes are refined by running a Monte Carlo simulation and rescored subsequently using GlideScore. GlideScore consists of (i) a lipophilic–lipophilic contact term, (ii) a H-bonding term, (iii) contributions from Coulomb and van der Waals interaction energies between ligand and the receptor, and (iv) a solvation model based on the computational interaction of explicit waters.

In the present work, the binding region of 1SMD was defined by a rectangular grid (14 Å × 12 Å × 14 Å) that was centered at  $X = 10.64$ ,  $Y = 15.71$ ,  $Z = 40.49$ , which corresponds to the position of the acarbose center of mass in 1CPU. For docking calculations, standard parameter settings were applied with the exception of the following: (i) extra precision (XP) docking was switched on; (ii) five- and six-membered rings were allowed to flip; and (iii) twisted (nonpolar) amide bonds were not penalized.

**FLO+ Docking.** FLO+ allows the study of interactions of fully flexible ligands with rigid, partially flexible, or fully flexible protein binding sites. By default, the software treats ligands as fully flexible and necessary constraints are imposed by internal molecular mechanics energy as well as the interaction energy with the protein. The size of a protein binding site can be defined by the user, and amino acids can be set to be rigid, partially flexible, or fully flexible. Ligand–protein interactions involve nonbonding molecular and superposition forces, the latter forces of which are automatically assigned on the basis of the chemical similarity of atoms and functional groups.

In this work, docking runs were centered on the C $\gamma$ -atom of Asp<sup>300</sup> in 1SMD (option SDOCK). For each ligand, 300 steps of Monte Carlo docking runs (option MCDOCK+) were calculated and the two top ranked poses were kept for further analysis. For the FLO+ docking runs the following 65 residues were allowed to move freely in 1SMD: Ile<sup>51</sup>, His<sup>52</sup>, Asn<sup>53</sup>, Pro<sup>54</sup>, Phe<sup>55</sup>, Arg<sup>56</sup>, Pro<sup>57</sup>, Trp<sup>58</sup>, Trp<sup>59</sup>, Glu<sup>60</sup>, Arg<sup>61</sup>, Tyr<sup>62</sup>, Gln<sup>63</sup>, Val<sup>98</sup>, Asn<sup>100</sup>, His<sup>101</sup>, Cys<sup>103</sup>, Gly<sup>104</sup>, Asn<sup>105</sup>, Ala<sup>106</sup>, Val<sup>107</sup>, Ser<sup>108</sup>, Ala<sup>109</sup>, Asp<sup>147</sup>, Ile<sup>148</sup>, Glu<sup>149</sup>, Asn<sup>150</sup>, Tyr<sup>151</sup>, Asn<sup>152</sup>, Arg<sup>161</sup>, Leu<sup>162</sup>, Ser<sup>163</sup>, Gly<sup>164</sup>, Leu<sup>165</sup>, Arg<sup>195</sup>, Asp<sup>197</sup>, Ala<sup>198</sup>, Ser<sup>199</sup>, Lys<sup>200</sup>, His<sup>201</sup>, Glu<sup>233</sup>, Val<sup>234</sup>, Ile<sup>235</sup>, Asp<sup>236</sup>, Leu<sup>237</sup>, Gly<sup>238</sup>, Gly<sup>239</sup>, Glu<sup>240</sup>, Pro<sup>241</sup>, Phe<sup>256</sup>, Lys<sup>257</sup>, Ala<sup>260</sup>, Lys<sup>261</sup>, Asn<sup>298</sup>, His<sup>299</sup>, Asp<sup>300</sup>, Asn<sup>301</sup>, Gly<sup>304</sup>, His<sup>305</sup>, Gly<sup>306</sup>, Ala<sup>307</sup>, Gly<sup>308</sup>, Gly<sup>309</sup>, Asp<sup>356</sup>, and Trp<sup>357</sup>.

**Acknowledgment.** The authors are most grateful to Colin McMartin and Regine S. Bohacek who generously enabled us to use FLO+ software for the purpose of our study.

## References

- (1) Henrissat, B. A classification of glycosyl hydrolases based on amino acid sequence similarities. *Biochem. J.* **1991**, *280* (Part 2), 309–316.
- (2) Brayer, G. D.; Sidhu, G.; Maurus, R.; Rydberg, E. H.; Braun, C.; Wang, Y.; Nguyen, N. T.; Overall, C. M.; Withers, S. G. Subsite mapping of the human pancreatic  $\alpha$ -amylase active site through structural, kinetic, and mutagenesis techniques. *Biochemistry* **2000**, *39*, 4778–4791.
- (3) Groot, P. C.; Bleeker, M. J.; Pronk, J. C.; Arwert, F.; Mager, W. H.; Planta, R. J.; Eriksson, A. W.; Frants, R. R. Human pancreatic amylase is encoded by two different genes. *Nucleic Acids Res.* **1988**, *16*, 4724.
- (4) Gumucio, D. L.; Wiebauer, K.; Caldwell, R. M.; Samuelson, L. C.; Meisler, M. H. Concerted evolution of human amylase genes. *Mol. Cell. Biol.* **1988**, *8*, 1197–1205.
- (5) Brayer, G. D.; Luo, Y.; Withers, S. G. The structure of human pancreatic  $\alpha$ -amylase at 1.8 Å resolution and comparisons with related enzymes. *Protein Sci.* **1995**, *4*, 1730–1742.
- (6) Ramasubbu, N.; Paloth, V.; Luo, Y.; Brayer, G. D.; Levine, M. J. Structure of human salivary  $\alpha$ -amylase at 1.6 Å resolution: implications for its role in the oral cavity. *Acta Crystallogr., Sect. D: Biol. Crystallogr.* **1996**, *52*, 435–446.
- (7) Al Kazaz, M.; Desseaux, V.; Marchis-Mouren, G.; Prodanov, E.; Santimone, M. The mechanism of porcine pancreatic  $\alpha$ -amylase. Inhibition of maltopentaose hydrolysis by acarbose, maltose and maltotriose. *Eur. J. Biochem.* **1998**, *252*, 100–107.
- (8) Kim, M. J.; Lee, S. B.; Lee, H. S.; Lee, S. Y.; Baek, J. S.; Kim, D.; Moon, T. W.; Robyt, J. F.; Park, K. H. Comparative study of the inhibition of  $\alpha$ -glucosidase,  $\alpha$ -amylase, and cyclomaltodextrin glucanotransferase by acarbose, isoacarbonyl, and acarviosine-glucose. *Arch. Biochem. Biophys.* **1999**, *371*, 277–283.
- (9) Lankisch, M.; Layer, P.; Rizza, R. A.; DiMaggio, E. P. Acute postprandial gastrointestinal and metabolic effects of wheat amylase inhibitor (WAI) in normal, obese, and diabetic humans. *Pancreas* **1998**, *17*, 176–181.
- (10) Boivin, M.; Flourie, B.; Rizza, R. A.; Go, V. L.; DiMaggio, E. P. Gastrointestinal and metabolic effects of amylase inhibition in diabetics. *Gastroenterology* **1988**, *94*, 387–394.
- (11) Kim, J. S.; Kwon, C. S.; Son, K. H. Inhibition of  $\alpha$ -glucosidase and amylase by luteolin, a flavonoid. *Biosci. Biotechnol. Biochem.* **2000**, *64*, 2458–2461.
- (12) McDougall, G. J.; Shpiro, F.; Dobson, P.; Smith, P.; Blake, A.; Stewart, D. Different polyphenolic components of soft fruits inhibit  $\alpha$ -amylase and  $\alpha$ -glucosidase. *J. Agric. Food Chem.* **2005**, *53*, 2760–2766.
- (13) Zhang, J.; Kashket, S. Inhibition of salivary amylase by black and green teas and their effects on the intraoral hydrolysis of starch. *Caries Res.* **1998**, *32*, 233–238.
- (14) He, Q.; Lv, Y.; Yao, K. Effects of tea polyphenols on the activities of  $\alpha$ -amylase, pepsin, trypsin and lipase. *Food Chem.* **2006**, *101*, 1178–1182.
- (15) Tadera, K.; Minami, Y.; Takamatsu, K.; Matsuoka, T. Inhibition of  $\alpha$ -glucosidase and  $\alpha$ -amylase by flavonoids. *J. Nutr. Sci. Vitaminol.* **2006**, *52*, 149–153.
- (16) Rydberg, E. H.; Li, C.; Maurus, R.; Overall, C. M.; Brayer, G. D.; Withers, S. G. Mechanistic analyses of catalysis in human pancreatic  $\alpha$ -amylase: detailed kinetic and structural studies of mutants of three conserved carboxylic acids. *Biochemistry* **2002**, *41*, 4492–4502.
- (17) O'Connor, C. M.; McGeeney, K. F. Interaction of human  $\alpha$ -amylases with inhibitors from wheat flour. *Biochim. Biophys. Acta* **1981**, *658*, 397–405.
- (18) Marshall, J. J.; Lauda, C. M. Purification and properties of phaseolamin, an inhibitor of  $\alpha$ -amylase, from the kidney bean, *Phaseolus vulgaris*. *J. Biol. Chem.* **1975**, *250*, 8030–8037.
- (19) Jia, W.; Gao, W.; Tang, L. Antidiabetic herbal drugs officially approved in China. *Phytother. Res.* **2003**, *17*, 1127–1134.
- (20) McCue, P.; Vatter, D.; Shetty, K. Inhibitory effect of clonal oregano extracts against porcine pancreatic amylase in vitro. *Asia Pac. J. Clin. Nutr.* **2004**, *13*, 401–408.
- (21) Starch blockers do not block starch digestion. *Nutr. Rev.* **1985**, *43*, 46–48.
- (22) Silano, V.; Furia, M.; Gianfreda, L.; Macri, A.; Palescandolo, R.; Rab, A.; Scardi, V.; Stella, E.; Valfre, F. Inhibition of amylases from different origins by albumins from the wheat kernel. *Biochim. Biophys. Acta* **1975**, *391*, 170–178.
- (23) O'Donnell, M. D.; McGeeney, K. F. Purification and properties of an  $\alpha$ -amylase inhibitor from wheat. *Biochim. Biophys. Acta* **1976**, *422*, 159–169.
- (24) Marais, J. P.; De Wit, J. L.; Quicke, G. V. A critical examination of the Nelson–Somogyi method for the determination of reducing sugars. *Anal. Biochem.* **1966**, *15*, 373–381.



- (25) Guex, N.; Peitsch, M. C. SWISS-MODEL and the Swiss-PdbViewer: an environment for comparative protein modeling. *Electrophoresis* **1997**, *18*, 2714–2723.
- (26) *Maestro*, version 7.5; Schrödinger LLC: Portland, OR, 2004.
- (27) Banks, J. L.; Beard, H. S.; Cao, Y.; Cho, A. E.; Damm, W.; Farid, R.; Felts, A. K.; Halgren, T. A.; Mainz, D. T.; Maple, J. R.; Murphy, R.; Philipp, D. M.; Repasky, M. P.; Zhang, L. Y.; Berne, B. J.; Friesner, R. A.; Gallicchio, E.; Levy, R. M. Integrated modeling program, applied chemical theory (IMPACT). *J. Comput. Chem.* **2005**, *26*, 1752–1780.
- (28) Halgren, T. A.; Murphy, R. B.; Friesner, R. A.; Beard, H. S.; Frye, L. L.; Pollard, W. T.; Banks, J. L. Glide: a new approach for rapid, accurate docking and scoring. 2. Enrichment factors in database screening. *J. Med. Chem.* **2004**, *47*, 1750–1759.
- (29) Friesner, R. A.; Banks, J. L.; Murphy, R. B.; Halgren, T. A.; Klicic, J. J.; Mainz, D. T.; Repasky, M. P.; Knoll, E. H.; Shelley, M.; Perry, J. K.; Shaw, D. E.; Francis, P.; Shenkin, P. S. Glide: a new approach for rapid, accurate docking and scoring. 1. Method and assessment of docking accuracy. *J. Med. Chem.* **2004**, *47*, 1739–1749.
- (30) Friesner, R. A.; Murphy, R. B.; Repasky, M. P.; Frye, L. L.; Greenwood, J. R.; Halgren, T. A.; Sanschagrin, P. C.; Mainz, D. T. Extra precision glide: docking and scoring incorporating a model of hydrophobic enclosure for protein-ligand complexes. *J. Med. Chem.* **2006**, *49*, 6177–6196.
- (31) McMartin, C.; Bohacek, R. S. QXP: powerful, rapid computer algorithms for structure-based drug design. *J. Comput.-Aided Mol. Des.* **1997**, *11*, 333–344.
- (32) Jorgensen, W. L.; Maxwell, D. S.; Tirado-Rives, J. Development and testing of the OPLS all-atom force field on conformational energetics and properties of organic liquids. *J. Am. Chem. Soc.* **1996**, *118*, 11225–11236.

JM800115X